1   **Title**

2   Arabidopsis Root-Type Ferredoxin:NADP(H) Oxidoreductase 2 Is Involved in

3   Detoxification of Nitrite in Roots

4

5   **Running head**

6   Detoxification of nitrite by root FNR2

7

8   **Corresponding author**

9   Takushi Hachiya

10   RIKEN Center for Sustainable Resource Science, 1-7-22 Suehiro-cho, Tsurumi-ku,

11   Yokohama, Kanagawa 230-0045, Japan

12   Fax: +81-45-503-9609

13   e-mail: hachiya.takushi@h.mbox.nagoya-u.ac.jp

14

15   **Subject areas**

16   (2) Environmental and stress responses

17

18   **Number of**

19   Black and white figures: 2

20   Color figures: 3

21   Tables: 0

22   Number of supplementary materials: 5

23 **Title**

24 Arabidopsis Root-Type Ferredoxin:NADP(H) Oxidoreductase 2 Is Involved in

25 Detoxification of Nitrite in Roots

26 **Running head**

27 Detoxification of nitrite by root FNR2

28 **Author**

29 Takushi Hachiya[1,2], Nanae Ueda[1], Munenori Kitagawa[3], Guy Hanke[4], Akira Suzuki[5],

30 Toshiharu Hase[6] and Hitoshi Sakakibara[1,2]

31 **Author's addresses**

32 [1]RIKEN Center for Sustainable Resource Science, 1-7-22 Suehiro-cho, Tsurumi-ku,

33 Yokohama, Kanagawa 230-0045, Japan, [2]Department of Biological Mechanisms and

34 Functions, Graduate School of Bioagricultural Sciences, Nagoya University, Nagoya,

35 Aichi 464-8601, Japan, [3]Cold Spring Harbor Laboratory, Cold Spring Harbor, New York

36 11724, [4]School of Biological and Chemical Sciences, Queen Mary University of London,

37 Mile End Road, 7 London E1 4NS, UK, [5]INRA, Institut Jean-Pierre Bourgin, UMR1318,

38 ERL CNRS 3559, Saclay Plant Sciences, RD10, F-78026 Versailles, France, [6]Laboratory

39 of Regulation of Biological Reaction, Institute for Protein Research, Osaka University,

40 Suita, Osaka, 565-0871 Japan

41 **Abbreviations**

42 FNR, ferredoxin:NADP(H) oxidoreductse; Fd, ferredoxin; G6PD, glucose-6-phosphate

43 dehydrogenase; GOGAT, glutamine-oxoglutarate aminotransferase; GS, glutamine

44 synthetase; GUS, β-glucuronidase; N, nitrogen; NiR, nitrite reductase; NO, nitric oxide;

45   NR, nitrate reductase; NRT, nitrate transporter; oxPPP, oxidative pentose phosphate

46   pathway; Q-PCR, quantitative reverse transcription polymerase chain reaction; RT-PCR,

47   reverse transcription polymerase chain reaction

48   **Footnotes**

49   The nucleotide sequence reported in this paper has been submitted to The Arabidopsis

50   Information Resource (TAIR) under accession numbers

51

52

53

54

55

56

57

58

59

60

61

62

63

64

65

66

Abstract

Ferredoxin : NADP(H) oxidoreductase (FNR) plays a key role in redox metabolism in plastids. Whereas leaf FNR (LFNR) is required for photosynthesis, root FNR (RFNR) is believed to provide electrons to ferredoxin (Fd)-dependent enzymes, including nitrite reductase (NiR) and Fd-glutamine-oxoglutarate aminotransferase (Fd-GOGAT) in non-photosynthetic conditions. In some herbal species, however, most nitrate reductase activity is located in photosynthetic organs, and ammonium in roots is assimilated mainly by Fd-independent NADH-GOGAT. Therefore, RFNR might have a limited impact on N assimilation in roots grown with nitrate or ammonium nitrogen sources. *AtRFNRs* are rapidly induced by application of toxic nitrite. Thus, we tested the hypothesis that RFNR could contribute to nitrite reduction in roots by comparing *A. thaliana* seedlings of wild type with loss-of-function mutants of *RFNR2*. When these seedlings were grown under nitrate, nitrite or ammonium, only nitrite nutrition caused impaired growth and nitrite accumulation in roots of *rfnr2*. Supplementation of nitrite with nitrate or ammonium as N sources did not restore the root growth in *rfnr2*. Also, a scavenger for nitric oxide (NO) could not effectively rescue the growth impairment. Thus, nitrite toxicity, rather than N depletion or nitrite-dependent NO production, probably causes the *rfnr2* root growth defect. Our results strongly suggest that RFNR2 has a major role in reduction of toxic nitrite in roots. A specific set of genes related to nitrite reduction and the supply of reducing power responded to nitrite concomitantly, suggesting that the products of these genes act cooperatively with RFNR2 to reduce nitrite in roots. (249 words)

4

89   isoform

90

91

92

93

94

95

96

97

98

99

100

101

102

103

104

105

106

107

108

109

110   **Introduction**

111   Ferredoxin : NADP(H) oxidoreductase (FNR) plays a key role in redox

112   metabolism in plastids (Hanke and Mulo 2013). In chloroplasts, FNR oxidizes the

113   reduced form of ferredoxin (Fd) to reduce $NADP^+$, which in turn, supplies the Calvin

114   cycle with NADPH. In non-photosynthetic plastids, FNR reduces Fd using NADPH

115   derived from the oxidative pentose phosphate pathway (oxPPP), providing reducing

116   power for various biosynthetic processes such as assimilatory pathways of nitrogen (N),

117   sulfur and fatty acids. These opposing reactions are believed to be catalyzed by specific

118   FNR isoproteins, i.e. leaf FNR (LFNR) and root FNR (RFNR), respectively (Hanke et al.

119   2004, Hanke et al. 2005). In *Arabidopsis thaliana*, loss-of-function of *AtLFNRs* impaired

120   autotrophic growth and photosynthetic capacity, demonstrating their essential roles in

121   operating the electron flow *in vivo* (Lintala et al. 2009, Lintala et al. 2012). By contrast,

122   the physiological importance of RFNR remains to be investigated using knock-out

123   mutants.

124   N assimilation requires a large amount of reducing power. The Fd-dependent

125   enzymes in this pathway include nitrite reductase (NiR) and Fd-glutamine-oxoglutarate

126   aminotransferase (Fd-GOGAT). Given that expression of *AtRFNRs* (*RFNR1*; At4g05390,

127   *RFNR2*; At1g30510, see Hanke et al. 2005) are induced by application of either nitrate or

128   ammonium (Wang et al. 2000, 2003, Patterson et al. 2010), AtRFNRs could provide

129   reducing equivalents to N assimilation in roots. In some herbal species, however, nitrate

130   is reduced predominantly in shoots using the reducing equivalents derived from

131   photosynthesis (Scheurwater et al. 2002, Bloom et al. 2010). Nitrate reductase (NR)

132   activities of hydroponically grown *A. thaliana* were much higher in shoots than roots

133   (Rachmilevitch et al. 2004, Krapp et al. 2011). Thus, RFNR may play a minor role in N

134   reduction in roots grown with nitrate. Ammonium addition to *Arabidopsis* roots induced

135   *NADH-GOGAT* rather than *Fd-GOGAT* expression in a concentration-dependent manner

136   (Konishi et al. 2014). Moreover, analyses with loss-of-function mutants have suggested

137   that NADH-GOGAT is the major enzyme converting ammonium-derived glutamine to

138   glutamate in roots (Lancien et al. 2002, Konishi et al. 2014). It is therefore doubtful that

139   RFNR supports nitrogen assimilation by furnishing Fd-GOGAT with reduced Fd in roots

140   grown with ammonium.

141   Recently, nitrite has been attracting attention as the third inorganic N source

142   (Kotur et al. 2013). Nitrite availability varies in the soil worldwide depending on the

143   balance between nitrification and denitrification (Samater et al. 1998, Riley et al. 2001,

144   Shen et al. 2003). Although nitrite concentrations in the soil are generally low compared

145   with nitrate and ammonium, a few hundred μM of nitrite have been detected in some soils

146   (Jones and Schwab 1993, López Pasquali et al. 2007). Nitrite can be taken up via different

147   pathways in *A. thaliana* (Kotur et al. 2013). One is mediated via active transporters

148   including high-affinity nitrate transporter 2 (NRT2), and another is simple diffusion of

149   nitrous acid under low pH. It is noteworthy that micromolar concentrations of nitrite act

150   as a signal to rapidly alter a genome-wide expression of numerous transcripts in *A.*

151   *thaliana* (Wang et al. 2007). The existence of functional machineries for nitrite uptake

152   and signaling suggests that nitrite could be an important N source for plants in the field.

153   Nitrite must be reduced immediately after its uptake, because of its high toxicity to plants.

154   In fact, *AtRFNRs* and *NIR* can be induced by application of   only 5 μM nitrite within 20

155   minutes (Wang et al. 2007). Therefore, we verified the hypothesis that RFNR could have

156   a major role in reducing environmental nitrite as N source using *A. thaliana* seedlings of

157   wild type (Col) and loss-of-function mutants of *RFNR*. Our results strongly suggest that

158   AtRFNR2 is essential for reduction and detoxification of nitrite absorbed by roots to

159   avoid accumulation of nitrite and the resultant defects in plant growth.

160

161

162

163

164

165

166

167

168

169

170

171

172

173

174

175

176   **Results**

177   *Identification of T-DNA insertion mutants of RFNR1 and RFNR2*

178   One T-DNA insertion allele for *RFNR1* (SALK_085009; *rfnr1*) and two

179   independent alleles for *RFNR2* (SAIL_527_G10.V1; *rfnr2-1*, SALK_133654; *rfnr2-2*)

180   were obtained from the European Arabidopsis Stock Centre (Fig. 1A). *rfnr1* and *rfnr2-1*

181   have T-DNA insertions in the second exon and in the first intron, respectively. An

182   insertion of T-DNA in *rfnr2-2* extends from the fourth exon to the fourth intron. We

183   checked mRNA levels of full-length *RFNRs* in roots of these lines with reverse

184   transcription PCR (RT-PCR) (Fig. 1B, Supplementary Fig. S1A). In *rfnr1* and *rfnr2-2*,

185   there was no transcript signal from the corresponding *RFNR* genes (Fig. 1B). On the other

186   hand, lower amounts of signals were detected in *rfnr2-1* than Col (Supplementary Fig.

187   S1A). A quantitative reverse transcription PCR (Q-PCR) analysis also revealed that

188   transcript levels of *RFNR2* in *rfnr2-1* accounted for about 18-25% of the transcript

189   amount in Col roots (Supplementary Fig. S1B). To determine protein content of RFNRs,

190   we conducted western analysis with the polyclonal antibody raised against a recombinant

191   maize RFNR (Onda et al. 2000). Two independent signals were observed in Col, where

192   the upper and lower bands correspond to RFNR1 and RFNR2, respectively (Hanke et al.

193   2005). In *rfnr1*, no upper signal was detected, whereas, in *rfnr2-1* and *rfnr2-2*, the lower

194   signal was absent (Fig. 1C, Supplementary S1C). We concluded that *rfnr1* and *rfnr2-2*

195   are knockout mutants and that *rfnr2-1* is a knockdown mutant.

196

197   *Expression of RFNR1 and RFNR2 under different N growth conditions*

198   To determine steady-state transcript levels of *RFNR1* and *RFNR2* under

199 different N sources, we conducted Q-PCR analysis using Col grown with 0.2 mM of

200 nitrate (NA), nitrite (NI) or ammonium (A) as the sole N source for seven days (Fig. 2A).

201 This N concentration is within the conceivable range in the field (Miller et al. 2007, Kotur

202 et al. 2013), and was sufficient to grow plants without causing N depletion (see protein

203 contents in plants in Fig. 4E). Irrespective of N source, both *RFNRs* were expressed

204 predominantly in roots (Fig. 2A), where the copy numbers of *RFNR2* mRNA were more

205 than ten times those of *RFNR1*. In the roots of Col grown with nitrite, a western analysis

206 also showed that RFNR2 had stronger signals than RFNR1 (Fig. 1C). The transcript levels

207 of *RFNR1* were similar among N conditions both in shoots and roots, whereas those of

208 *RFNR2* attained the maximum level in the roots grown with nitrite.

209 Nitrate and nitrite application can induce expression of a large number of genes

210 in tens of minutes (Wang et al. 2003, Wang et al. 2007, Patterson et al. 2010). To analyze

211 the short-term N responses, we grew seedlings for seven days under ammonium

212 conditions and transferred them into fresh media containing nitrate, nitrite or ammonium

213 as the sole N source. *RFNR2* expression levels in roots were compared before and after a

214 30 minute incubation with each N source (Fig. 2B). *RFNR2* was significantly induced by

215 nitrite addition, but not by nitrate or ammonium. In the present study, we focused on

216 RFNR2 as the major isoform responding to nitrite-supplied conditions.

217 To monitor a tissue-specific pattern of transcriptional activity for *RFNR2*, we

218 generated transgenic plants with β-glucuronidase (GUS) fused to the region between –

219 879 and +24 bp from the first ATG codon of *RFNR2* (For details, see Materials and

220 methods). The T_3 homozygous transgenic plants were grown for five days under nitrate

10

221   or nitrite, and blue GUS signals were observed with a stereoscopic microscope (Fig. 2C)

222   and an optical microscope (Fig. 2D, E). Under both N sources, the signals were localized

223   predominantly in roots, consistent with the Q-PCR observations (Fig. 2A, C). Basal

224   regions of primary roots had stronger signals than root tips (Fig. 2C). In the middle region

225   of the primary root, vascular bundles were remarkably stained, although the outer layer

226   of cells also showed weaker GUS signals (Fig. 2D). Strong signals were also observed in

227   the columella cells of root tips (Fig. 2E). Overall, the signal intensities of GUS were

228   higher under nitrite than nitrate (Fig. 2C-E), which also corresponded to the tendency

229   observed with Q-PCR (Fig. 2A, B). Both transcript levels of authentic *RFNR2* and

230   heterologous *GUS* driven by the *RFNR2* promoter were higher in 5-day-old roots under

231   nitrite (Fig. 2F), suggesting that the nitrite induction of *RFNR2* is under transcriptional

232   control.

233

234   *Root growth of rfnr2 mutants on different N sources*

235   Next, we compared root growth between Col and *rfnr2* mutants to elucidate

236   whether RFNR2 could contribute to nitrite reduction (Fig. 3, Supplementary Fig. S1D-

237   F). In Col, the length of primary roots was slightly, but significantly, longer under nitrate

238   growth conditions than with nitrite or ammonium (Fig. 3A, B, Supplementary Fig. S1D,

239   E). Primary root growth of *rfnr2-2* decreased relative to Col under nitrite growth

240   conditions, whereas, under nitrate or ammonium condition, no significant difference was

241   observed. Also, in *rfnr2-1*, primary root length was shorter under nitrite, but not under

242   nitrate. The length of lateral roots was also longest in Col supplied with nitrate, followed

243   in order by nitrite and ammonium (Fig. 3A, C, Supplementary Fig. S1D, F). Relative to

244   Col, *rfnr2-2* showed remarkably stunted growth of lateral roots under nitrite growth

245   conditions, although the mutant also had a slight decrease in lateral root length under

246   nitrate conditions (Fig. 3C). In *rfnr2-1*, however, no significant decrease in lateral root

247   length was observed (Supplementary Fig. S1F).

248   We then investigated root growth in the knockout mutant, *rfnr2-2*, in detail. To

249   determine the effective concentration of nitrite that results in primary root defects in

250   *rfnr2-2*, we analyzed the concentration-dependence of primary root elongation on nitrate

251   or nitrite at 0, 0.04, 0.2 and 1 mM (Fig. 3D). Little difference in primary root length was

252   observed between Col and *rfnr2-2* under nitrate growth conditions at any concentration.

253   By contrast, nitrite caused primary root elongation defects in *rfnr2-2* plants at 0.04, 0.2

254   and 1 mM. The extent of this defect in root growth increased with the nitrite

255   concentration. It should be noted that primary root lengths in *rfnr2-2* were shorter under

256   nitrite than under no N condition, suggesting that the stunted root phenotype is primarily

257   due to a detrimental effect of nitrite on root growth, rather than an inability to assimilate

258   N in the roots.

259   A time-course analysis revealed that, on nitrite supply, daily primary root

260   elongation in *rfnr2-2* was severely suppressed at early stages of development (4-6 d), and

261   that the suppression tended to be mitigated at later stages (7-9 d) (Fig. 3E).

262   To validate whether the root growth defects of *rfnr2-2* plants grown on nitrite

263   persist, we transferred 4-day-old seedlings grown on either nitrate or nitrite to fresh

264   medium containing different N sources. The seedlings were grown for three further days,

265 and their primary root elongation during the period after transfer was determined (Fig.

266 3F). Irrespective of the N source before the transfer, the *rfnr2-2* transferred to nitrite

267 condition showed stunted primary root growth. On the other hand, the transfer from nitrite

268 to nitrate conditions restored the rate of primary root elongation. These data suggest that

269 the defective phenotype of the mutant is reversible.

270

271 *Exploring the causes of root growth defects in rfnr2*

272   If RFNR2 contributes to nitrite reduction in roots, its deficiency should cause

273 nitrite accumulation therein. To confirm this, we measured nitrite concentrations in roots

274 of 7-day-old plants grown under nitrate or nitrite (Fig. 4A). Under nitrite conditions, more

275 than 100 nmol g fresh weight^{-1} of nitrite was determined in *rfnr2-2* roots, whereas nitrite

276 was not significantly detected in Col roots. Nitrite also accumulated in the roots of *rfnr2-*

277 *1*, although the extent was less than in *rfnr2-2* (Supplementary Fig. S1G). In roots of

278 plants grown with nitrate, no significant amount of nitrite was detected in either Col or

279 *rfnr2-2* (Fig. 4A), indicating that any contribution of RFNR2 to N assimilation in

280 Arabidopsis is redundant. Excess accumulation of nitrite is frequently accompanied by

281 nitric oxide (NO) biosynthesis via a side reaction catalyzed by nitrate reductase (NR)

282 (Rockel et al. 2002, Wang et al. 2007), which may inhibit primary root growth

283 (Fernández-Marcos et al. 2012). Thus, we checked whether a NO scavenger could restore

284 primary root growth in *rfnr2-2* roots grown with nitrite (Fig. 4B). However, application

285 of 200 μM of carboxy-PTIO did not affect the phenotype in *rfnr2-2*. Likewise, the

286 transcript level of an NO-inducible marker gene, *AOX1a* (Huang et al. 2002), was

287 unaffected by *RFNR2* deficiency (Fig. 4C). Furthermore, we could not detect NR activity

288 in nitrite-grown Col roots, whilst, in the shoots, 8.27 ± 1.53 nmol g FW^{-1} min^{-1} of NR

289 activity was measured (Fig. 4D). Taken together, the data contradict any contribution of

290 NO to root growth defects in the *RFNR2* mutants.

291   Severe N depletion decreases primary root growth in *A. thaliana* (Araya et al.

292 2014), providing another possible explanation for the *rfnr2* phenotype: *RFNR2* deficiency

293 may deplete total N assimilation when nitrite is supplied as the sole N source. We

294 therefore measured protein amounts in 7-day-old seedlings of Col and *rfnr2-2* (Fig. 4E),

295 but could not observe any significant decrease in protein content of *rfnr2-2* seedlings,

296 indicating that NiR activity in the leaves, supported by photosynthesis, is sufficient for N

297 assimilation. Moreover, additional application of 0.2 mM nitrate or 0.2 mM ammonium

298 to 0.2 mM nitrite (i.e. 0.4 mM N included in the media) did not restore the wild type root

299 phenotype in *rfnr2-2* (Fig. 4F, G). In addition, as demonstrated in Fig.3D, primary root

300 lengths in *rfnr2-2* were even shorter with nitrite than under no N growth conditions. These

301 observations suggest that toxicity of nitrite *per se* could suppress root growth in *rfnr2-2*,

302 and that the impairment of root growth is not due to N deprivation.

303

304 *Identification of genes acting with RFNR2 in nitrite detoxification*

305   To provide reducing power for efficient nitrite reduction in roots, NIR, RFNR,

306 Fd and oxPPP would have to respond to nitrite concomitantly (see Introduction). To

307 identify a set of additional, specifically relevant genes, we surveyed genes co-expressed

308 with *RFNR2* using the ATTED II program (Obayashi et al. 2014). Supplementary Table

309 S1 shows a list of genes within the ranking's top ten. This includes one *NIR* (*NIR*;

310 At2g15620), one root type *FD* (*FD3*; At2g27510) and one *FNR* (*RFNR1*; At4g05390). In

311 the oxPPP, two *GLUCOSE-6-PHOSPHATE DEHYDROGENASEs* (*G6PD2;* At5g13110,

312 *G6PD3*; At1g24280), two putative *6-PHOSPHOGLUCONATE DEHYDROGENASEs*

313 (At1g64190, At5g41670) and one *TRANSALDOLASE* (*TRA2*; At5g13420) were

314 identified. We analyzed whether *NIR*, *FD3*, *RFNR1*, *G6PD2*, *G6PD3*, *At1g64190* and

315 *At5g41670* could respond to different N sources in the same way as *RFNR2* (Fig. 5A, B).

316 Under steady-state growth conditions, all these genes were expressed predominantly in

317 roots, and their expression levels attained the maximum in roots grown with nitrite (Fig.

318 5A). On the other hand, expression of the reference gene *At4g34270* (Hong et al. 2010)

319 was not significantly different between N sources in shoots or roots (Fig. 5A). Short-term

320 analysis also revealed that induction of the above genes was consistently strongest

321 following nitrite application, whereas expression of *At4g34270* was not significantly

322 changed (Fig. 5B). This expression response pattern is similar to that of *RFNR2* (Fig. 2A,

323 B), suggesting that the products of these genes act cooperatively with RFNR2 to form an

324 electron supply system for nitrite reduction in roots. If this hypothesis is correct, nitrite

325 induced expression of these genes would be enhanced in the *RFNR2* mutants as

326 compensation. As expected, the steady-state transcript levels were higher in *rfnr2-2* roots

327 under nitrite growth conditions (Fig. 5C), while *At4g34270* expression was affected little

328 by *RFNR2* deficiency. A similar tendency was found in *rfnr2-1*, although the extent of

329 compensation was less than in *rfnr2-2* (Supplementary Fig. S1H).

330

331   *Verifying the role of RFNR2 with nitrate or ammonium as N sources*

332   We found little difference in root growth between Col and *RFNR2* mutants

333   under nitrate or ammonium growth conditions (Fig. 3, Supplementary Fig. S1D, E). This

334   means that RFNR2 may only play a minor role in N assimilation from these N sources,

335   as mentioned in the Introduction. In short, we assume that in *A. thaliana*, nitrate reduction

336   and the subsequent Fd-dependent steps occur mainly in shoots, and that ammonium

337   absorbed by the roots is assimilated into glutamine by GS in the roots, followed by its

338   conversion to glutamate mainly by NADH-GOGAT.

339   If nitrate was reduced predominantly in shoots, NR activity would be higher in

340   shoots than roots. Indeed, in seedlings grown with nitrate, an abundant activity of NR was

341   detected in shoots, but no significant activity was detected in roots (Fig. 6A, for

342   comparison, see Yu et al. 1998, Konishi and Yanagisawa 2011). In a NR double mutant

343   (*nr*) grown in the presence of nitrate, more nitrate was accumulated in shoots relative to

344   Col, but not in roots (Fig. 6B), confirming that nitrate reduction occurs mainly in shoots

345   *in vivo*. Furthermore, in Figure 4A, *RFNR2* deficiency did not affect nitrite concentrations

346   in roots under nitrate growth conditions, suggesting that nitrite was scarcely produced in

347   the roots grown with nitrate.

348   *GLN1;2* is an ammonium-inducible isoform of GS expressed in the root

349   vasculature (Ishiyama et al. 2004, Konishi et al. 2014, Guan et al. 2015). Our Q-PCR

350   analysis revealed that *GLN1;2* was expressed predominantly in roots, and attained

351   maximum expression levels under ammonium growth conditions (Supplementary Fig.

352   S2A). On the other hand, transcripts of *GLN2*, the plastidic isoform of GS, were much

16

353 higher in shoots than roots. Total GS activities are almost comparable between shoots and

354 roots (Supplementary Fig. S2B). In roots, the highest activity was observed under

355 ammonium growth conditions, followed by nitrite and then nitrate conditions,

356 corresponding to the expression pattern of *GLN1;2* (Supplementary Fig. S2A, B). A

357 knockout of *GLN1;2* (*gln1;2*, Lothier et al. 2011) decreased root GS activity by ca. 35%

358 of Col (Fig. 6C). More ammonium was accumulated in the *gln1;2* roots grown with

359 ammonium than Col (Fig. 6D). Furthermore, *gln1;2* showed impaired lateral root growth

360 under ammonium (Supplementary Fig. S2C). These observations indicate that a

361 significant portion of ammonium absorbed by roots is normally assimilated in the root.

362 Following ammonium incorporation into glutamine, the subsequent conversion of

363 glutamine to glutamate can be catalyzed by Fd-GOGAT (*GLU1*, *GLU2*) or NADH-

364 GOGAT (*GLT*). Q-PCR analysis showed that, of these three genes, *GLU2* and *GLT* were

365 predominantly expressed in roots (Supplementary Fig. S2D). If RFNR2 contributes to

366 glutamate biosynthesis under ammonium growth conditions, the contents of glutamine

367 and glutamate in the roots would be expected to change on *RFNR2* deficiency. The results,

368 however, show that there is no significant difference in either amino acid between Col

369 and *rfnr2-2* (Fig. 6E). Moreover, no compensatory induction of *RFNR1*, *FD3*, *G6PD3*,

370 *At5g41670*, *GLT* or *GLU2* expression occurred in *rfnr2-2* grown with ammonium

371 (Supplementary Fig. S2E). These results suggest that RFNR2 does not make a significant

372 contribution to glutamate biosynthesis under ammonium growth conditions. Taken

373 together, we conclude that RFNR2 has a significant role in N reduction/assimilation of

374 nitrite, rather than nitrate or ammonium.

375

376   **Discussion**

377   Plants use nitrate and ammonium as major N sources (Kiba and Krapp 2016).

378   Currently, these are recognized as not only substrates for protein synthesis but also signals

379   that alter gene expression and root morphology (Remans et al. 2006, Lima et al. 2010,

380   Patterson et al. 2010). To date, the components for their transport and signaling have been

381   comprehensively identified and characterized (Krapp et al. 2015). On the other hand, far

382   less information about nitrite is available, although measurable amounts of nitrite are

383   often present in the soil and can accumulate to high levels depending on pH (Shen et al.

384   2003, Kotur et al. 2013). Nitrite is actively taken up by specific transport systems and

385   used for N assimilation (Kotur et al. 2013). Plants can sense exogenous nitrite at

386   micromolar concentrations, and respond by altering their transcriptome (Wang et al.

387   2007). There is no doubt that nitrite is a third inorganic N source worthy of attention. NiR

388   is the sole enzyme for nitrite reduction and is completely dependent on the reduced form

389   of ferredoxin as an electron donor. In *NIR* antisense tobacco plants, growth is suppressed

390   with accompanying accumulation of nitrite to extremely high concentrations (Morot-

391   Gaudry-Talarmain et al. 2002). Our results suggest that in *rfnr2* mutants NiR can not

392   fulfill its physiological role in roots due to a limitation in electron supply.

393   The data presented here indicate that in Arabidopsis, both NO_3 and NH_4, but

394   not NO_2, are primarily transported to the shoot for assimilation. If such a mechanism

395   were also applied to NO_2, the plant would be subject to severe toxic effects. To avoid this,

396   NO_2 assimilation depends on an effective electron supply to NiR by RFNR in the root, in

397 order to reduce NO_2 to NH_4 before transport to the leaf.

398   Here we provide strong evidence supporting the hypothesis that *in vivo* the flux

399 rate of nitrite reduction is decreased in the *RFNR2* mutants as the system for supplying

400 reduced Fd to NiR is disrupted. However, testing this hypothesis directly is

401 experimentally problematic using the conventional method of assaying NiR activity. In

402 this method, maximum activity of NiR is measured with an excess amounts of electron

403 donors. Thus, it would not reflect *in vivo* flux rate of nitrite reduction, and any defect in

404 NiR reduction due to impaired electron supply would not be detected. It is therefore a

405 research priority to develop a new method for quantitative evaluation of the flux rate in

406 the future.

407   Primary root growth of two *RFNR2* mutants decreased relative to Col under

408 nitrite growth conditions, whereas only *rfnr2-2* showed the stunted growth of lateral roots

409 under nitrite. This phenotypic discrepancy may reflect the extent of genetic defects (i.e.

410 knockout in *rfnr2-2*, knockdown in *rfnr2-1*). We concluded that *RFNR2* deficiency

411 impacts on primary root growth when nitrite is supplied as the N source.

412   Given that nitrite is toxic, its conversion to organic N results in detoxification.

413 Since nitrite reduction occurs only in plastids, this toxic nitrite should be promptly

414 transported into plastids before its reduction. In *A. thaliana*, specific transporters for

415 nitrite uptake into plastids have been identified as *NITR2;1* and *NITR2;2* (Maeda et al.

416 2014). The promoter-directed GUS signal of *NITR2;2* was detected exclusively in roots.

417 An *in silico* survey for the genes co-expressed with *RFNR2* found that *NITR2;2* was

418 ranked 13th (Obayashi et al. 2014). NITR2;2 may therefore be important for the

419   immediate reduction of nitrite taken up from the soil.

420   Our expression analysis confirmed that *AtRFNR1* was expressed at a lower

421   level than *AtRFNR2*, and AtRFNR1 is a minor form (Fig. 1C, 2A). It is possible that

422   RFNR1 has some redundant function with RFNR2 in roots, because *RFNR1* showed a

423   similar expression pattern to *RFNR2* in response to different N sources (Fig. 5B) and

424   *RFNR1* was induced in *rfnr2-2* in a compensatory manner (Fig. 5C). Interestingly, the

425   suppression of primary root elongation in *rfnr2-2* was mitigated at its later growth stages

426   under nitrite growth conditions (Fig. 3E), indicating that *RFNR1* might partly alleviate

427   nitrite accumulation and its toxicity in *rfnr2-2*, although the compensation was not

428   sufficient to completely restore the root growth (Fig. 3). On the other hand, root growth

429   of a *RFNR1* knockout mutant was not impaired under nitrite growth conditions

430   (Supplementary Fig. S3A-C). The contribution of RFNR1 to reduction of nitrite absorbed

431   by roots is therefore probably limited.

432   The genes coexpressed with *RFNR2* in Figure 5 have all been identified as both

433   nitrate- and nitrite-inducible genes (Supplemental Data in Wang et al. 2007). In this case,

434   we observed that nitrite induced much stronger effects on gene expression than nitrate

435   (Fig. 5A, B). A uniform response of the genes indicates strict control of expression by a

436   single mechanism that originates with nitrite perception. Both expression of *NIR* and

437   *NITR2;2* are under the control of the NIN-like protein (NLP) family of transcription

438   factors, responding to nitrate *per se* (Konishi and Yanagisawa 2013, Maeda et al. 2014).

439   A mutation of the nitrate sensor *CHL1/NRT1.1/NPF6.3* suppressed nitrate induction of

440   genes related to nitrite detoxification examined in Figure 5 (Supplemental Data in Wang

441 et al. 2009). Considering that over one-half of nitrite-responding genes overlap with

442 nitrate-responding genes (Wang et al. 2007) and that the molecular structure of nitrate

443 and nitrite is similar, it is possible that the same components could be involved in both

444 nitrate signaling and the nitrite induction of these genes.

445   In *A. thaliana*, chloroplasts purified from *LFNR1* knockout plants had enhanced

446 activities of nitrite reduction compared with those from Col (Hanke et al. 2008). This

447 implies a competition for reduced Fd between LFNR and NIR. Bloom et al. (2010) have

448 demonstrated that, in leaves, the conversion from nitrate to ammonium is suppressed

449 under elevated CO_2 with nitrate as an N source. This suggests that increased demand on

450 NADPH for CO_2 assimilation in the Calvin Benson cycle could deplete the reduced leaf

451 Fd available for NIR. Thus, some leaf localized Fd-dependent enzymatic reactions may

452 be limited by electron supply under high CO_2, which in turn, could   necessitate a greater

453 contribution of root localized Fd-dependent reactions to bioassimilatory and biosynthetic

454 processes. Enhanced CO_2 assimilation under high CO_2 has been shown to increase

455 carbon partitioning to roots (Duan et al. 2014), providing more sugar for NADPH

456 production in the oxPPP. Reduction of root Fd by RFNR is a future research target worthy

457 of attention in the context of increasing CO_2 concentrations in the atmosphere.

458

459

460

461

462

463

464

465

466

467

468

469

470

471

472

Materials and Methods

Plant materials and growth conditions

Arabidopsis thaliana (L.) Heynh. accession Col and mutants *rfnr1*-KO (SALK_085009),

rfnr2-KO (SALK_133654), *rfnr2*-KD (SAIL_527_G10), *gln1;2*-KO (SALK_102291,

Lothier et al. 2011) and *nia1-1nia2-5* (*nr*), a *NITRATE REDUCTASE* double mutant

(Wilkinson and Crawford 1993) were used in our experiments. The seeds were purchased

from the European Arabidopsis Stock Centre. After surface sterilization, 10 seeds were

sown on plastic Petri dishes (length 140 mm, width 100 mm, depth 20 mm; Eiken Kagaku,

Tokyo, Japan) containing 50 ml of half-strength Murashige and Skoog-macro- and micro-

nutrient salts (except for N) with 0.05% (w/v) MES-H_2O, 1% (w/v) sucrose (Murashige

and Skoog 1962). For the media containing 0.2 mM of nitrate (NA), nitrite (NI) or

ammonium (A), 0.2 mM KNO_3 and 1.8 mM KCl, 0.2 mM KNO_2 and 1.8 mM KCl or 0.2

485   mM NH_4Cl and 2 mM KCl were added, respectively. The media were solidified with

486   0.5% (w/v) gerangum, and pH of the media was adjusted to 6.15 with KOH. After sowing,

487   the plates were kept at 4°C in the dark for three days. Plants were grown in a vertical

488   position on plastic dishes under a photosynthetic photon flux density of 100–120 μmol

489   m^{-2} s^{-1} (16 h light/8 h dark cycle) at 23°C. Ten seeds per plate were sown in all

490   experiments. For comparisons between Col and mutants, five seeds of each line were

491   placed on the same plate, if not specified. Further details are given in the Results and

492   figure legends.

493

494   *Root growth analysis*

495   For analysis of root growth, 7-day-old plants were harvested and scanned at

496   300 dpi resolution for measurement of root length according to Hachiya et al. (2014). The

497   root architecture was traced using Photoshop Elements 11 (Adobe Systems), and the

498   lengths of primary and lateral roots were measured from traced images using ImageJ

499   software (ver.1.47).

500

501   *Preparation for segmented plates*

502   A localized addition of nitrate or nitrite to plants was accomplished using

503   segmented plates where two patches were separated by an air gap (Remans et al. 2006).

504   For preparation of the segmented plate, basic nutrient media (as described above)

505   containing no N sources were solidified. The narrow gel split was eliminated with sterile

506   razors and forceps to create an air gap. Subsequently, concentrated potassium nitrate or

507   potassium nitrite were placed and spread on each patch of the media. To allow

508   homogenous diffusion of the N sources, the plated were prepared more than 48 h before

509   the experiments. Three 4-day-old Col and *rfnr2-2* plants of each line grown on 0.2 mM

510   of ammonium medium were transferred onto the segmented plates. It should be noted that

511   shoots and roots were in contact with only the upper and lower patches, respectively. The

512   plants were grown for a further three days, and elongation of the primary root was

513   measured as described above.

514

515   *Extraction of total RNA, reverse transcription and real-time PCR*

516   For purification of total RNA, shoots or roots were harvested, immediately

517   frozen with liquid N_2 and stored at $-80°C$ before use. All samples per plate were regarded

518   as one biological replicate. Frozen samples were ground with a TissueLyser II (QIAGEN,

519   Hilden, Germany) using 5 mm zirconia beads. Total RNA was extracted using RNeasy

520   plant mini kit (QIAGEN) according to the manufacturer's instructions with on-column

521   DNase digestion. Reverse transcription was performed with a ReverTra Ace qPCR RT

522   Master Mix (Toyobo Life Science, Tokyo, Japan) according to the manufacturer's

523   instructions. The synthesized cDNA was diluted 10-fold with distilled water for real-time

524   PCR.

525   Transcript levels were measured using a StepOnePlus Real-Time PCR System

526   (ThermoFisher Scientific, Waltham, MA, USA). cDNA (2 µl) was amplified in the

527   presence of 10 µl of KAPA SYBR FAST qPCR Kit (Nippon Genetics Co., Ltd., Tokyo,

528   Japan), 0.5 µl of specific primers (0.2 µM final concentration) and 7.5 µl sterilized water.

529 Transcript levels were quantified using absolute or relative standard curve with *ACTIN3*

530 as the internal standard. Plasmid DNA containing the corresponding cDNAs or total

531 cDNAs were used as templates to generate standard curves. Primer sequences used for

532 the experiments are shown in Supplemental Table S2. Primers were designed with the

533 NCBI/Primer-BLAST program.

534

535 *Western analysis of RFNR proteins*

536 Roots were harvested, immediately frozen with liquid N_2 and stored at $-80°C$

537 before use. All samples per two plates were regarded as one biological replicate. Frozen

538 samples were ground with a TissueLyser II (QIAGEN) using 5 mm zirconia beads. Total

539 proteins were extracted with 10 volumes of sample buffer (NuPAGE LDS Sample buffer

540 and NuPAGE Reducing Agent, ThermoFisher Scientific) followed by incubation at 95˚C

541 for 5 min. The extracts were centrifuged at 20,400 *g* at room temperature for 10 min. 10

542 µl of the supernatant was subjected to SDS-PAGE in a 15% (w/v) gel and transferred to

543 a PVDF membrane (Immobilon-P, Merck Millipore, Darmstadt, Germany) at 2 mA cm^{-2}

544 for 1.5 h in transfer buffer (NuPAGE Transfer Buffer, ThermoFisher Scientific). The

545 membrane was incubated in blocking buffer containing ECL Prime Blocking Agent (GE

546 Healthcare, Little Chalfont, UK), 0.02% Tween-20, 20 mM Tris-HCl, pH 7.4, 140 mM

547 NaCl for 1 h, and reacted with a 1/50000 dilution of the polyclonal antibody raised against

548 maize RFNR overnight (Onda et al. 2000). After rinsing, the antigen-antibody complex

549 was detected by 1/50000 dilution of horseradish peroxidase (HRP)-conjugated with goat

550 antibody against rabbit IgG (NA935, GE Healthcare) and visualized by chemiluminescent

551   detection (ECL Prime, GE Healthcare) using ImageQuant LAS 4010 (GE Healthcare).

552

553   *Determination of nitrate, nitrite, ammonium, glutamine, glutamate and protein*

554   Nitrate was extracted and determined according to Hachiya et al. (2012) with

555   slight modifications. Shoots or roots were harvested and dried at 80°C before use. All

556   samples per plate were regarded as one biological replicate. Nitrate was extracted with

557   10 volumes of water at 100°C for 10 min. 10 µl of supernatant was mixed with 40 µl of

558   reaction reagent (50 mg salicylic acid per one ml concentrated sulfuric acid), and the

559   mixture was incubated at room temperature for 20 min. For the mock treatment, 40 µl of

560   concentrated sulfuric acid only was added to 10 µl of supernatant. After an addition of 1

561   ml of NaOH to the mixture, absorbance at 410 nm was scanned. Nitrate content of the

562   supernatant was calculated based on standard curve with dilution series of potassium

563   nitrate.

564   For nitrite determination, roots were harvested, immediately frozen with liquid

565   N_2 and stored at −80°C before use. All samples per five plates were regarded as one

566   biological replicate. Frozen samples were ground with a TissueLyser II (QIAGEN) using

567   5 mm zirconia beads. Nitrite was extracted with 5 volumes of extraction buffer (50 mM

568   Hepes-KOH, pH7.6, 1 mM EDTA, 7 mM cysteine). The extracts were centrifuged at

569   20,400 *g* at 4°C for 10 min. The supernatant was mixed with equal volumes of 1% (w/v)

570   sulfanilamide solution in 1N HCl and 0.02% (w/v) N-1-Naphthylethylenediamine

571   dihydrochloride solution in H_2O. For detection of the nonspecific background, 1% (w/v)

572   sulfanilamide solution in 1N HCl was replaced by 1N HCl. The mixture was incubated at

573 room temperature for 15 min followed by scanning absorbance at 540 nm. Nitrite content

574 of the supernatant was calculated based on standard curve with dilution series of

575 potassium nitrite by subtracting the background values from the total values.

576   For ammonium determination, roots were harvested, immediately frozen with

577 liquid N_2 and stored at −80°C before use. All samples per plate were regarded as one

578 biological replicate. Ammonium was extracted and determined according to Bräutigam

579 et al. (2007) with slight modifications. Frozen samples were ground with a TissueLyser

580 II (QIAGEN) using 5 mm zirconia beads. 1 ml of 0.1 N HCl and 500 µl of chloroform

581 were added to the frozen powder. The mixture was rotated for 15 min at 4°C followed by

582 centrifugation at 12,000 g at 8°C for 10 min. The aqueous phase was further purified by

583 acid-washed activated charcoal (No. 035-18081; Wako, Osaka, Japan). Ammonium

584 content of the supernatant was spectroscopically determined using an ammonia test kit

585 (No. 277-14401, Wako) according to the manufacturer's instructions.

586   For determination of glutamine and glutamate, roots were harvested,

587 immediately frozen with liquid N_2 and stored at −80°C before use. All samples per five

588 plates were regarded as one biological replicate. Glutamine and glutamate were extracted

589 and determined according to Kamada-Nobusada et al. (2013). Frozen samples were

590 ground with a TissueLyser II (QIAGEN) using 5 mm zirconia beads. The powder was

591 mixed with 10 volumes of 10 mM HCl containing 0.2 mM methionine sulfone as an

592 internal control. The homogenate was centrifuged at 20400 g at 4°C for 5 min, and the

593 supernatant was filtered through Ultrafree-MC filters (No. UFC30GV00, Merck

594 Millipore). Amino acid contents in the resulting filtrate were determined using Pico-Tag

595 (Waters Corporation, Milford, MA, USA) with an HPLC System (Waters Alliance 2695

596 HPLC system/2475) according to the manufacturer's instructions.

597   Total protein was extracted as described above. 10 µl of the extracts were

598 suspended into 500 µl of H_2O, after which 100 µl of 0.15 % (w/v) sodium deoxycholate

599 aqueous solution was added, and the mixture was incubated at room temperature for 10

600 min. Subsequent addition of 100 µl of 72% (v/v) trichloroacetic acid was followed by

601 incubation at room temperature for 15 min. The mixture was centrifuged at 20,400 g at

602 room temperature for 10 min, and the precipitates were dried at room temperature and

603 used for protein determination by a BCA method (Takara BCA Protein Assay Kit No.

604 T9300A, Takara Bio Inc., Otsu, Japan) according to the manufacturer's instructions.

605

606 *Determination of activities of nitrate reductase and glutamine synthetase*

607   NR activity was determined according to Konishi and Yanagisawa (2011).

608 Shoots or roots were harvested, immediately frozen with liquid N_2 and stored at −80°C

609 before use. All samples per two plates were regarded as one biological replicate. Frozen

610 samples were ground with a TissueLyser II (QIAGEN) using 5 mm zirconia beads. The

611 powder was mixed with 5 volumes of extraction buffer (50 mM Hepes-KOH, pH7.6, 1

612 mM EDTA, 7 mM cysteine). The extracts were centrifuged at 20,400 g at 4°C for 10 min.

613 25 µl of the supernatant was added to 75 µl of assay buffer (50 mM Hepes-KOH, pH7.6,

614 100 µM NADH, 2 mM EDTA, 5 mM KNO_3). After incubation at 30°C for 15 min, nitrite

615 produced was determined as mentioned above.

616   GS activity was determined as the ADP-dependent conversion rate of L-

617   glutamine to γ-glutamylhydroxamate according to Taira et al. (2004) and Li et al. (2012)

618   with slight modifications. Shoots or roots were harvested, immediately frozen with liquid

619   N_2 and stored at −80°C before use. All samples per two plates were regarded as one

620   biological replicate. Frozen samples were ground with a TissueLyser II (QIAGEN) using

621   5 mm zirconia beads. The powder was mixed with 10 volumes of extraction buffer (100

622   mM Tris-HCl, pH7.5, 1% (w/v) PVP-40, 1 mM EDTA, 1 mM $MnCl_2$, 0.5% (v/v) β-

623   mercaptoethanol, 0.1 mM APMSF). The extracts were centrifuged at 12,000 g at 4°C for

624   10 min. 45 µl of assay buffer (40 mM imidazole-HCl, pH 7.0, 20 mM sodium arsenate,

625   0.5 mM ADP, 3 mM $MnCl_2$, 60 mM NH_2OH, 30 mM L-glutamine) was added to 5µl of

626   the supernatant, and the mixture was incubated at 30°C for 15 min. Reactions were

627   stopped by adding 30 µl of $FeCl_3$-TCA-HCl solution (2.6% $FeCl_3 \cdot 6H_2O$, 4%

628   trichloroacetic acid in 1N HCl). The products were measured by absorbance at 540 nm.

629

630   *Construction of ProRFNR2:GUS fusions*

631   The putative promoter region (–879 to +24 bp from the first ATG codon) was

632   amplified from *Arabidopsis* genomic DNA using PrimeSTAR GXL DNA Polymerase

633   (Takara Bio Inc.) and specific primers (see Supplemental Table 2). PCR products were

634   cloned into pENTR using pENTR/D-TOPO Cloning Kit (ThermoFisher Scientific)

635   according to the manufacturer's instructions, sequenced, and subcloned into pBA002a-

636   GW-GUS (Kiba et al. 2007) by LR reaction. The binary vector was transformed into

637   *Agrobacterium* strain EHA101. Transformants were selected on LB medium containing

638   100 mg L^{-1} spectinomycin and positive clones were recovered. *Arabidopsis* plants

639 accession Col was transformed by the floral dip method (Clough and Bent 1998).

640 Transgenic seedlings were isolated on Murashige and Skoog medium containing 1%

641 sucrose and 5 mg L^{-1} bialaphos sodium salt. Segregation ratios were analyzed to select

642 plants with one copy of T-DNA and to isolate homozygous plants. T3-homozygous plants

643 were used for experiments.

644

645 *GUS Staining*

646 Histochemical GUS staining was performed according to Jefferson (1987) with

647 slight modifications. Plants were incubated in 90% (v/v) acetone solution on ice for 15

648 min, and submerged into assay buffer (100 mM sodium phosphate, pH 7.4, 10 mM EDTA,

649 5 mM ferro/ferricyanide, 0.1% (v/v) Triton X-100, 0.5 mg mL^{-1} X-Gluc), followed by

650 vacuum infiltration at room temperature for 15 min. Plants were incubated in the dark at

651 37 ˚C for 4.5 h. The stained plants were washed with 70 % (v/v) ethanol and bleached

652 with 6:1 (v/v) ethanol : acetic acid. The samples were mounted with chloral hydrate

653 solution (8:1:2 (w/v/v) chloral hydrate : glycerol : H_2O) and observed using a

654 stereoscopic microscope (Olympus SZX12, Olympus, Tokyo, Japan) and an optical

655 microscope (Olympus BX53).

656

657 *Statistical analysis*

658 All statistical analyses were conducted using the R software package (ver.

659 2.15.3). Details of analyses are given in the Results and in table and figure legends.

660

661

662

663

664

665

666

667

Disclosures

Conflicts of interest: No conflicts of interest declared.

677

678

679

680

681

682

683

684

685

686

687

688

References

Andrew, M., Morton, J.D., Liefering, M. and Bisset, L. (1992) The partitioning of nitrate

assimilation between root and shoot of a range of temperate cereals and pasture grasses.

Ann. Bot. 70: 271-276.

Aoki, Y., Okamura, Y., Tadaka, S., Kinoshita, K. and Obayashi, T. (2016) ATTED-II in

2016: a plant coexpression database towards lineage-specific coexpression. *Plant Cell

Physiol.* Doi: 10.1093/pcp/pcv165.

Araya, T., Miyamoto, M., Wibowo, J., Suzuki, A., Kojima, S., Tsuchiya, Y.N., Sawa, S.,

Fukuda, H., von Wirén, N. and Takahashi, H. (2014) CLE-CLAVATA1 peptide-receptor

signaling module regulates the expansion of plant root systems in a nitrogen-dependent

manner. *Proc. Natl. Acad. Sci. USA* 111: 2029-2034.

Bloom, A.J., Burger, M., Asensio, J.S.R. and Cousins, A.B. (2010) Carbon dioxide

enrichment inhibits nitrate assimilation in wheat and *Arabidopsis*. *Science* 328: 899-903.

705

706 Bräutigam, A., Gagneul, D. and Weber, A.P.M. (2007) High-throughput colorimetric

707 method for the parallel assay of glyoxylic acid and ammonium in a single extract. *Anal.*

708 *Biochem.* 362: 151–153.

709

710 Clough, S.J. and Bent, A.F. (1998) Floral dip: a simplified method for *Agrobacterium-*

711 mediated transformation of *Arabidopsis thaliana*. *Plant J.* 16: 735-743.

712

713 Duan, Z., Homma, A., Kobayashi, M., Nagata, N., Kaneko, Y., Fujiki, Y. and Nishida, I.

714 (2014) Photoassimilation, assimilate translocation and plasmodesmal biogenesis in the

715 source leaves of *Arabidopsis thaliana* grown under an increased atmospheric CO_2

716 concentration. *Plant Cell Physiol.* 55: 358-369.

717

718 Fernández-Marcos, M., Sanz, L. and Lorenzo, O. (2012) An emerging regulator of cell

719 elongation during primary root growth. *Plant Signal. Behav.* 7: 196-200.

720

721 Guan, M., Møller, I.S. and Schjoerring, J.K. (2015) Two cytosolic glutamine synthetase

722 isoforms play specific roles for seed germination and seed yield structure in *Arabidopsis*.

723 *J. Exp. Bot.* 66: 203-212.

724

725 Hachiya, T., Watanabe, C.K., Fujimoto, M., Ishikawa, T., Takahara, K., Kawai-Yamada,

726 M. et al. (2012) Nitrate addition alleviates ammonium toxicity without lessening

727 ammonium accumulation, organic acid depletion and inorganic cation depletion in

728 Arabidopsis thaliana shoots. *Plant Cell Physiol*. 53: 577–591.

729

730 Hachiya, T., Sugiura, D., Kojima, M., Sato, S., Yanagisawa, S., Sakakibara, H.,

731 Terashima, I. and Noguchi, K. (2014) High CO_2 triggers preferential root growth of

732 Arabidopsis thaliana via two distinct systems under low pH and low N stresses. *Plant*

733 *Cell Physiol*. 55: 269–280.

734

735 Hanke, G.T., Kimata-Ariga, Y., Taniguchi, I. and Hase, T. (2004) A post genomic

736 characterization of Arabidopsis ferredoxins. *Plant Physiol.* 134: 255-264.

737

738 Hanke, G.T., Okutani, S., Satomi, Y., Takao, T., Suzuki, A. and Hase, T. (2005) Multiple

739 iso-proteins of FNR in *Arabidopsis*: evidence for different contributions to chloroplast

740 function and nitrogen assimilation. *Plant Cell Environ.* 28: 1146-1157.

741

742 Hanke, G.T. and Mulo, P. (2013). Plant type ferredoxins and ferredoxin-dependent

743 metabolism. *Plant Cell Environ.* 36: 1071-1084.

744

745 Hong, S.M., Bahn, S.C., Lyu, A., Jung, H.S. and Ahn, J.H. (2010) Identification and

746 testing of superior reference genes for a starting pool of transcript normalization in

747 Arabidopsis. *Plant Cell Physiol.* 51: 1694-1706.

748

749   Huang, X., von Rad, U. and Durner, J. (2002) Nitric oxide induces transcriptional

750   activation of the nitric oxide-tolerant alternative oxidase in *Arabidopsis* suspension cells.

751   *Planta* 215: 914-923.

752

753   Ishiyama, K., Inoue, E., Watanabe-Takahashi, A., Obara, M., Yamaya, T. and Takahashi,

754   H. (2004) Kinetic properties and ammonium-dependent regulation of cytosolic

755   isoenzymes of glutamine synthetase in *Arabidopsis*. *J. Biol. Chem.* 279: 16598-16605.

756

757   Jefferson, R.A. (1987) Assaying chimeric genes in plants: the GUS gene fusion system.

758   *Plant Mol. Biol. Rep.* 5: 387-405.

759

760   Jones, R.D. and Schwab, A.P. (1993) Nitrate leaching and nitrite occurrence in a fine-

761   textured soil. *Soil Sci.* 155: 272-281.

762

763   Kamada-Nobusada, T., Makita, N., Kojima, M. and Sakakibara, H. (2013) Nitrogen-

764   dependent regulation of de novo cytokinin biosynthesis in rice: the role of glutamine

765   metabolism as an additional signal. *Plant Cell Physiol.* 54: 1881–1893.

766

767   Kiba, T., Henriques, R., Sakakibara, H. and Chua, N.H. (2007) Targeted   degradation of

768   PSEUDO-RESPONSE REGULATOR5 by a SCFZTL complex regulates clock function

769   and photomorphogenesis in Arabidopsis thaliana. *Plant Cell* 19 : 2516

770

771   Kiba, T. and Krapp, Anne. (2016) Plant nitrogen acquisition under low availability:

772   regulation of uptake and root architecture. *Plant Cell Physiol.* Doi: 10.1093/pcp/pcw052

773

774   Konishi, M. and Yanagisawa, S. (2011) The regulatory region controlling the nitrate-

775   responsive expression of a nitrate reductase gene, *NIA1*, in Arabidopsis. *Plant Cell*

776   *Physiol.* 52: 824-836.

777

778   Konishi, M. and Yanagisawa, S. (2013) Arabidopsis NIN-like transcription factors have

779   a central role in nitrate signaling. *Nat. Commun.* 4: 1617.

780

781   Konishi, N., Ishiyama, K., Matsuoka, K., Maru, I., Hayakawa, T., Yamaya, T. and Kojima,

782   S. (2014) NADH-dependent glutamate synthase plays a crucial role in assimilation

783   ammonium in the Arabidopsis root. *Physiol. Plant* 152: 138-151.

784

785   Kotur, Z., Siddiqi, Y.M. and Glass, A.D.M. (2013) Characterization of nitrite uptake in

786   *Arabidopsis thaliana*: evidence for a nitrite-specific transporter. *New Phytol.* 200: 201-

787   210.

788

789   Krapp, A., Berthomé, R., Orsel, M., Mercey-Boutet, S., Yu, A., Castaings, L., Elftieh, S.,

790   Major, H., Renou, J.-P. and Daniel-Vedele, F. (2011) Arabidopsis roots and shoots show

791   distinct temporal adaptation patterns toward nitrogen starvation. *Plant Physiol.* 157:

792   1255-1282.

793

794 Krapp, A. (2015) Plant nitrogen assimilation and its regulation: a complex puzzle with

795 missing pieces. *Curr. Opin. Plant Biol.* 25: 115-122.

796

797 Lancien, M., Martin, M., Hsieh, M.-H., Leustek, T., Goodman, H. and Coruzzi, G. (2002)

798 Arabidopsis *glt1*-T mutant defines a role for NADH-GOGAT in the non-photorespiratory

799 ammonium assimilatory pathway. *Plant J.* 29: 347-358.

800

801 Li, G., Dong, G., Li, B., Li, Q., Kronzucker, H.J. and Shi, W. (2012) Isolation and

802 characterization of a novel ammonium overly sensitive mutant, amos2, in Arabidopsis

803 thaliana. *Planta* 235: 239-252.

804

805 Lindermayr, C., Saalbach, G. and Durner, J. (2005) Proteomic identification of S-

806 nitrosylated proteins in Arabidopsis. *Plant Physiol.* 137: 921-930.

807

808 Lima, J.E., Kojima, S., Takahashi, H. and von Wirén, N. (2010) Ammonium triggers

809 lateral root branching in *Arabidopsis* in an AMMONIUM TRANSPORTER1;3-

810 dependent manner. *Plant Cell* 22: 3621-3633.

811

812 Lintala, M., Allahverdiyeva, Y., Kangasjärvi, S., Lehtimäki, N., Keränen, M., Rintamäki,

813 E., Aro, E.-M. and Mulo, P. (2009) Comparative analysis of leaf-type ferredoxin-NADP$^+$

814 oxidoreductase isoforms in *Arabidopsis thaliana*. *Plant J* 57: 1103-1115.

815

816 Lintala, M., Lehtimäki, N., Benz, J.P., Jungfer, A., Soll, J., Aro, E.-M., Bölter, B. and

817 Mulo, P. (2012) Depletion of leaf-type ferredoxin-NADP$^+$ oxidoreductase results in the

818 permanent induction of photoprotective mechanisms in Arabidopsis chloroplasts. *Plant*

819 *J.* 70: 809-817.

820

821 López Pasquali, C.E., Fernández Hernando, P. and Durand Alegría, J.S. (2007)

822 Spectrophotometric simultaneous determination of nitrite, nitrate and ammonium in soils

823 by flow injection analysis. *Anal. Chim. Acta* 600: 177-182.

824

825 Lothier, J., Gaufichon, L., Sormani, R., Lemaître, T., Azzopardi, M., Morin, H., Chardon,

826 F., Reisdorf-Cren, M., Avice, J.-C. and Masclaux-Daubresse, C. (2011) The cytosolic

827 glutamine synthetase GLN1;2 plays a role in the control of plant growth and ammonium

828 homeostasis in *Arabidopsis* rosettes when nitrate supply is not limiting. *J. Exp. Bot.* 62:

829 1375-1390.

830

831 Maeda, S.-I., Konishi, M., Yanagisawa, S. and Omata, T. (2014) Nitrite transport activity

832 of a novel HPP family protein conserved in cyanobacteria and chloroplasts. *Plant Cell*

833 *Physiol.* 55: 1311-1324.

834

835 Miller, A.J., Fan, X., Orsel, M., Smith, S.J. and Wells, D.M. (2007) Nitrate transport and

836 signaling. *J. Exp. Bot.* 58: 2297-2306.

837

838   Murashige, T. and Skoog, F. (1962) A revised medium for rapid growth and bio assays

839   with tobacco tissue cultures. *Physiol. Plant.* 15: 473-497.

840

841   Obayashi, T., Okamura, Y., Ito, S., Tadaka, S., Aoki, Y., Shirota, M. and Kinoshita, K.

842   (2014) ATTED-II in 2014: Evaluation of gene coexpression in agriculturally important

843   plants. *Plant Cell Physiol.* 55: e6(1-7).

844

845   Onda, Y., Matsumura, T., Kimata-Ariga, Y., Sakakibara, H., Sugiyama, T. and Hase, T.

846   (2000) Differential interaction of maize root ferredoxin:NADP$^+$ oxidoreductase with

847   photosynthetic and non- photosynthetic ferredoxin isoproteins. *Plant Physiol.* 123: 1037-

848   1046.

849

850   Patterson, K., Cakmak, T., Cooper, A., Lager, I., Rasmusson, A.G. and Escobar, M.A.

851   (2010) Distinct signaling pathways and transcriptome response signatures differentiate

852   ammonium- and nitrate-supplied plants. *Plant Cell Environ.* 33: 1486-1501.

853

854   Rachmilevitch, S., Cousins, A.B. and Bloom, A.J. (2004) Nitrate assimilation in plant

855   shoots depends on photorespiration. *Proc. Natl. Acad. Sci. USA* 101: 11506-11510.

856

857   Remans, T., Nacry, P., Pervent, M., Filleur, S., Diatloff, E., Mounier, E., Tillard, P., Forde,

858   B.G. and Gojon, A. (2006) The *Arabidopsis* NRT1.1 transporter participates in the

859 signaling pathway triggering root colonization of nitrate-rich patches. *Proc. Natl. Acad.*

860 *Sci. USA* 103: 19206-19211.

861

862 Riley, W.J., Ortiz-Monasterio, I. and Matson, P.A. (2001) Nitrogen leaching and soil

863 nitrate, nitrite, and ammonium levels under irrigated wheat in Northern Mexico. *Nutr.*

864 *Cycl. Agroecosys.* 61: 223-236.

865

866 Rockel, P., Strube, F., Rockel, A., Wildt, J. and Kaiser, W.M. (2002) Regulation of nitric

867 oxide (NO) production by plant nitrate reductase *in vivo* and *in vitro*. *J. Exp. Bot.* 53: 103-

868 110.

869

870 Samater, A.H., Van Cleemput, O. and Ertebo, T. (1998) Influence of the presence of

871 nitrite and nitrate in soil on maize biomass production, nitrogen immobilization and

872 nitrogen recovery. *Biol. Fertil. Soils* 27: 211-218.

873

874 Scheurwater, I., Koren, M., Lambers, H. and Atkin, O.K. (2002) The contribution of roots

875 and shoots to whole plant nitrate reduction in fast- and slow-growing grass species. *J.*

876 *Exp. Bot.* 53: 1635-1642.

877

878 Shen, Q.R., Ran, W. and Cao, Z.H. (2003) Mechanisms of nitrite accumulation occurring

879 in soil nitrification. *Chemosphere* 50: 747-753.

880

881   Taira, M., Valtersson, U., Burkhardt, B. and Ludwig, R.A. (2004) *Arabidopsis thaliana*

882   *GLN2*-encoded glutamine synthetase is dual targeted to leaf mitochondria and

883   chloroplasts. *Plant Cell* 16 :2048-2058.

884

885   Wang, R., Guegler, K., LaBrie, S.T. and Crawford, N.M. (2000) Genomic analysis of a

886   nutrient response in Arabidopsis reveals diverse expression patterns and novel metabolic

887   and potential regulatory genes induced by nitrate. *Plant Cell* 12: 1491-1509.

888

889   Wang, R., Okamoto, M., Xing, X. and Crawford, N.M. (2003) Microarray analysis of the

890   nitrate response in Arabidopsis roots and shoots reveals over 1,000 rapidly responding

891   genes and new linkages to glucose, trehalose-6-phosphate, iron, and sulfate metabolism.

892   *Plant Physiol.* 132: 556-567.

893

894   Wang, R., Xing, X. and Crawford, N. (2007) Nitrite acts as a transcriptome signal at

895   micromolar concentrations in Arabidopsis roots. *Plant Physiol.* 145: 1735-1745.

896

897   Wang, R., Xing, X., Wang, Y., Tran, A. and Crawford, N.M. (2009) A genetic screen for

898   nitrate regulatory mutants captures the nitrate transporter gene NRT1.1. *Plant Physiol.*

899   151: 472-478.

900

901   Wilkinson, J.Q. and Crawford, N.M. (1993) Identification and characterization of a

902   chlorate-resistant mutant of *Arabidopsis thaliana* with mutations in both nitrate reductase

903   structural genes *NIA1* and *NIA2*. *Mol. Gen. Genet.* 239: 289-297.

904

905   Yu, X., Sukumaran, S. and Márton, L. (1998) Differential expression of the Arabidopsis

906   *Nia1* and *Nia2* genes. *Plant Physiol.* 116: 1091-1096.

907

908

909

910

911

912

913

914

915

916

917

918

919

920

921

922

923

924

925

926

927

928 **Legends to figures**

929 **Fig. 1** RFNR2 is the major RFNR isoform in roots grown on nitrite media. (A) Schematic

930 representation of *rfnr1* and *rfnr2* T-DNA insertion alleles. Boxes represent exons;

931 horizontal thin bars, untranslated region; horizontal thick bars, introns; ATG, initiation

932 codon; TGA, termination codon. (B) RT-PCR analysis using specific primers of *RFNR1*

933 and *RFNR2* transcript levels in roots of Col, *rfnr1* and *rfnr2-2* mutants grown under 0.2

934 mM nitrite for seven days (Supplementary Table S2). *ACT2* was used as the loading

935 control. (C) Immunodetection of RFNR1 and RFNR2 isoproteins with specific antisera

936 raised against maize RFNR following SDS-PAGE and western blotting in roots of Col,

937 *rfnr1* and *rfnr2-2* mutants grown under 0.2 mM nitrite for seven days. The position of the

938 nearest molecular weight marker is given on the left.

939

940 **Fig. 2** *RFNR2* is induced by nitrite. (A) Absolute transcript levels of *RFNR1* and *RFNR2*

941 in shoots and roots of Col grown under 0.2mM of nitrate (NA), nitrite (NI) or ammonium

942 (A) for seven days (Mean ± SD, n = 3). (B) Relative transcript levels of *RFNR2* in 7 d

943 Col roots before (0 min) or after (30 min) the transfer to 0.2 mM nitrate, nitrite or

944 ammonium (Mean ± SD, n = 3). (C) The tissue specific pattern of GUS activity in 5-day-

945 old *pRFNR2::GUS* seedlings grown under nitrate or nitrite. The arrowheads indicate root

946 tips. The scale bar denotes 10 mm. (D) GUS activity in the central portion of the primary

43

947   root. The scale bar denotes 100 μm. (E) GUS activity in the primary root tips. The scale

948   bar denotes 50 μm. (F) Relative transcript levels of *RFNR2* and *GUS* in the roots of 5 d

949   *pRFNR2::GUS* seedlings grown under nitrate or nitrite (Mean ± SD, n = 4). Tukey-

950   Kramer's multiple comparison test was conducted at a significance level of $P < 0.05$ only

951   when a one-way ANOVA was significant at $P < 0.05$. Different letters denote significant

952   differences. Student's *t*-test was conducted (*$P < 0.05$).

953

954   **Fig. 3** *RFNR2* is essential for normal root growth on nitrite media. (A) Representative

955   photographs in 9-day-old Col and *rfnr2-2* grown on media containing 0.2 mM nitrate,

956   nitrite or ammonium. (B) Primary root length in 7-day-old Col and *rfnr2-2* grown on 0.2

957   mM nitrate (NA), nitrite (NI) or ammonium (A) (Mean ± SD, n = 10). White and black

958   bars denote Col and *rfnr2-2*, respectively. (C) Lateral root length in 7-day-old Col and

959   *rfnr2-2* grown on 0.2 mM nitrate, nitrite or ammonium (Mean ± SD, n = 10). (D)

960   Concentration dependency of primary root length in 7-day-old Col and *rfnr2-2* grown on

961   0, 0.04, 0.2 and 1 mM nitrate or nitrite (Mean ± SD, n = 12-15). (E) Time-courses of

962   primary root elongation per day on 0.2 mM of each N source (Mean ± SD, n = 15). (F)

963   Primary root elongation 3 days after the transfer from 0.2 mM nitrate or nitrite to 0.2 mM

964   of nitrate or nitrite in 4-day-old Col and *rfnr2-2*. "NA to NA" means the transfer from 0.2

965   mM nitrate to 0.2 mM nitrate (Mean ± SD, n = 5). Tukey-Kramer's multiple comparison

966   test was conducted at a significance level of $P < 0.05$ only when a one-way ANOVA was

967   significant at $P < 0.05$. Different letters denote significant differences. NS means not

968   significant.

969

970 **Fig. 4** Impaired root growth of *RFNR2* mutant is due to nitrite accumulation. (A) Nitrite

971 contents in roots of 7-day-old Col and *rfnr2-2* grown on 0.2 mM nitrate (NA) or nitrite

972 (NI) (Mean ± SD, n = 3). White and black bars denote Col and *rfnr2-2*, respectively. (B)

973 Primary root length in 7-day-old Col and *rfnr2-2* grown on 0.2 mM nitrite in the presence

974 or absence of the NO scavenger, cPTIO (Mean ± SD, n = 10). (C) Relative transcript

975 levels of *AOX1a* in roots of 7-day-old Col and *rfnr2-2* grown on 0.2 mM nitrate or nitrite

976 (Mean ± SD, n = 3). (D) NR activities (NRA) in shoots and roots of 7-day-old Col grown

977 on 0.2 mM nitrite (Mean ± SD, n = 3). (E) Protein contents in plants of 7-day-old Col and

978 *rfnr2-2* grown on 0.2 mM nitrate, nitrite or ammonium (Mean ± SD, n = 3). (F) Primary

979 root length in 7-day-old Col and *rfnr2-2* under 0.2 mM of nitrate, 0.2 mM nitrate plus 0.2

980 mM nitrite (i.e. 0.4 mM N in total), 0.2 mM nitrite, 0.2 mM nitrite plus 0.2 mM of

981 ammonium (i.e. 0.4 mM N in total) or 0.2 mM ammonium (Mean ± SD, n = 10). (G)

982 Representative photographs in 7-day-old Col and *rfnr2-2* grown on 0.2 mM nitrate, 0.2

983 mM nitrate plus 0.2 mM nitrite or 0.2 mM nitrite. Tukey-Kramer's multiple comparison

984 test was conducted at a significance level of $P < 0.05$ only when a one-way ANOVA was

985 significant at $P < 0.05$. Different letters denote significant differences. ND and NS mean

986 not detected and not significant, respectively.

987

988 **Fig. 5** A specific set of genes related to nitrite reduction uniformly responds to nitrite. (A)

989 Relative transcript levels of *NIR*, *FD3*, *G6PD2*, *G6PD3*, *At1g64190*, *At5g41670* and

990 *At4g34270* (a reference gene, Hong et al. 2010) in shoots and roots of 7-day-old Col

45

991   grown on 0.2mM nitrate (NA), nitrite (NI) or ammonium (A) for seven days (Mean ± SD,

992   n = 3). (B) Relative transcript levels of *NIR*, *FD3*, *G6PD2*, *G6PD3*, *At1g64190*,

993   *At5g41670*, *RFNR1* and *At4g34270* in 7-day-old Col roots before (0 min) or after (30

994   min) transfer to 0.2 mM nitrate, nitrite or ammonium (Mean ± SD, n = 3). (C) Relative

995   transcript levels of *NIR*, *FD3*, *G6PD2*, *G6PD3*, *At1g64190*, *At5g41670*, *RFNR1* and

996   *At4g34270* in roots of 7-day-old Col and *rfnr2-2* grown on 0.2mM nitrite (Mean ± SD, n

997   = 3). White and black bars denote Col and *rfnr2-2*, respectively. Tukey-Kramer's multiple

998   comparison test was conducted at a significance level of $P < 0.05$ only when a one-way

999   ANOVA was significant at $P < 0.05$. Student's *t*-test was conducted (*P < 0.05). NS

1000   means not significant.

1001

1002   **Fig. 6** RFNR2 is not essential for N reduction/assimilation when nitrate or ammonium

1003   are the sole N sources. (A) NR activities (NRA) in shoots and roots of 7-day-old Col on

1004   0.2 mM nitrate (Mean ± SD, n = 4). (B) Nitrate contents in shoots and roots of 7-day-old

1005   Col and NR double mutant (*nr*) on 0.2 mM nitrate (Mean ± SD, n = 3). White and dotted

1006   bars denote Col and *nr*, respectively. (C) GS activities in roots of 7-day-old Col and *gln1;2*

1007   grown on 0.2mM ammonium (Mean ± SD, n = 4). White and diagonal bars denote Col

1008   and *gln1;2*, respectively. (D) Ammonium contents in the roots of 7-day-old Col and

1009   *gln1;2* grown on 0.2 mM ammonium (Mean ± SD, n = 3). (E) Contents of glutamine and

1010   glutamate in roots of 7-day-old Col and *rfnr2-2* grown on 0.2 mM ammonium (Mean ±

1011   SD, n = 3). White and black bars denote Col and *rfnr2-2*, respectively. Tukey-Kramer's

1012   multiple comparison test was conducted at a significance level of $P < 0.05$ only when a

46

1013   one-way ANOVA was significant at $P < 0.05$. Different letters denote significant

1014   differences. Student's t-test was conducted (*$P < 0.05$). ND and NS mean not detected

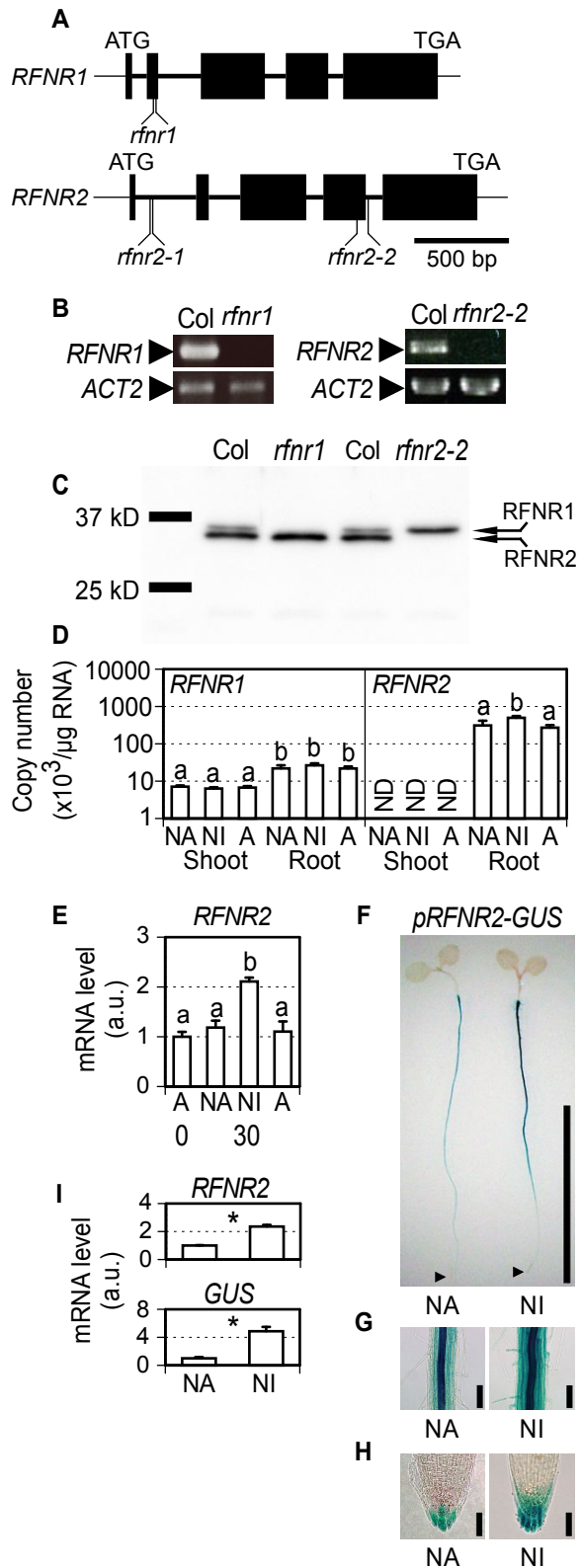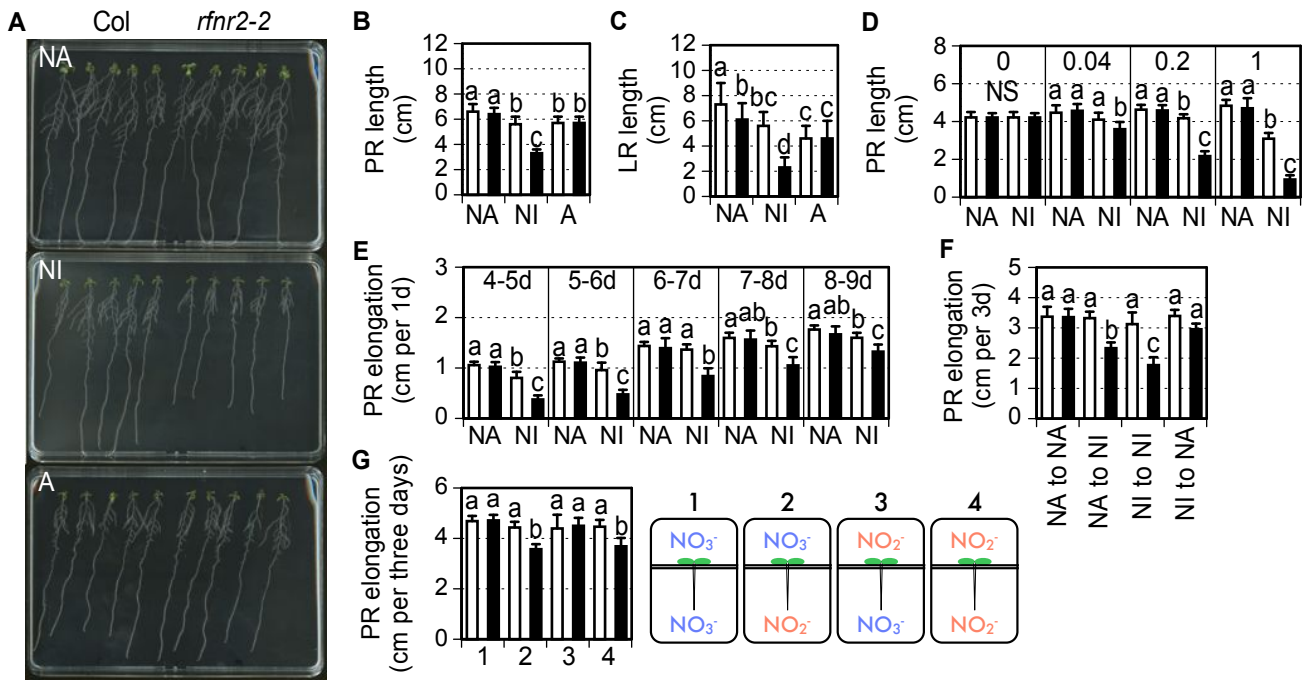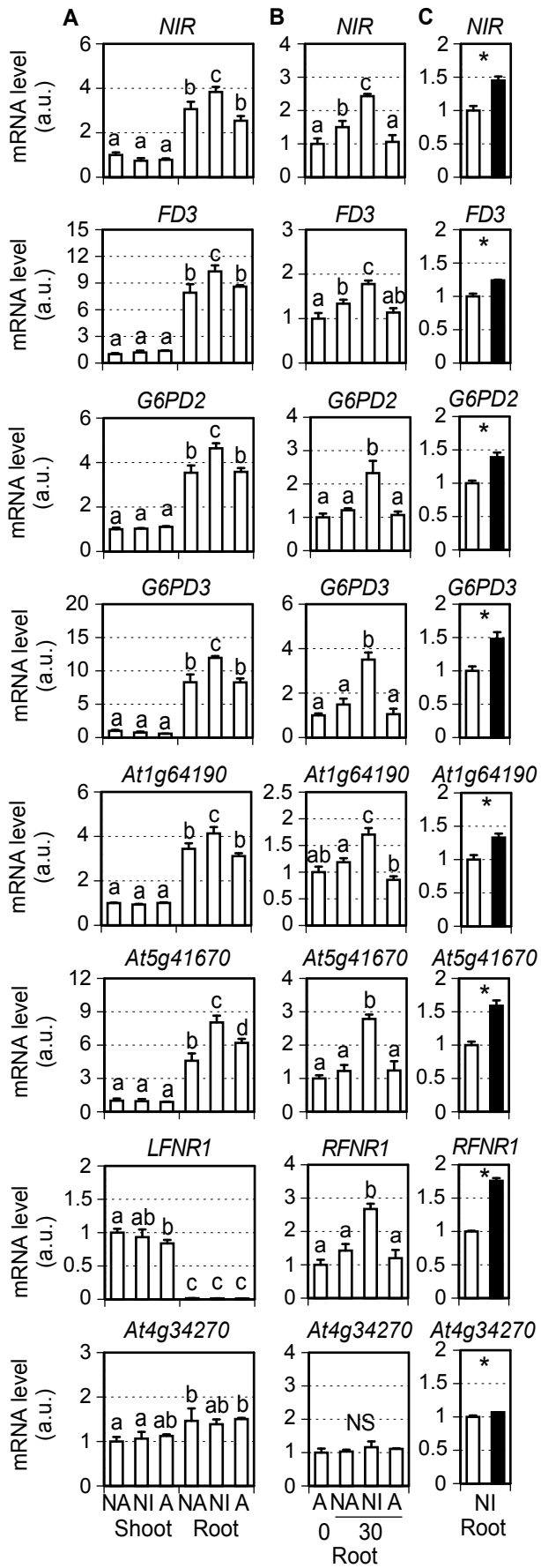1015   and not significant, respectively.

Figure 1

A

ATG   TGA
RFNR1 ━━┃▮━━▮▮━━▮━━▮━━
        rfnr1

ATG   TGA
RFNR2 ━━▮━━▮━▮▮━━▮━▮━━
     rfnr2-1   rfnr2-2
                              500 bp

B

           Col rfnr1   Col rfnr2-2
RFNR1 ▶   RFNR2 ▶
ACT2 ▶   ACT2 ▶

C

        Col   rfnr1   Col   rfnr2-2
37 kD ━   ← RFNR1
                                     ← RFNR2
25 kD ━

D

RFNR1   RFNR2
Copy number (×10³/µg RNA)

a a a   b b b   ND ND ND a b a
NA NI A NA NI A   NA NI A   NA NI A
 Shoot   Root   Shoot   Root

E

RFNR2
mRNA level (a.u.)
a a   b a
A NA NI A
0   30

F   pRFNR2-GUS

NA   NI

G

NA   NI

H

NA   NI

I

RFNR2
mRNA level (a.u.)
        *
NA   NI

GUS
        *
NA   NI

Figure 2

Figure 3

Figure 4

Figure 5

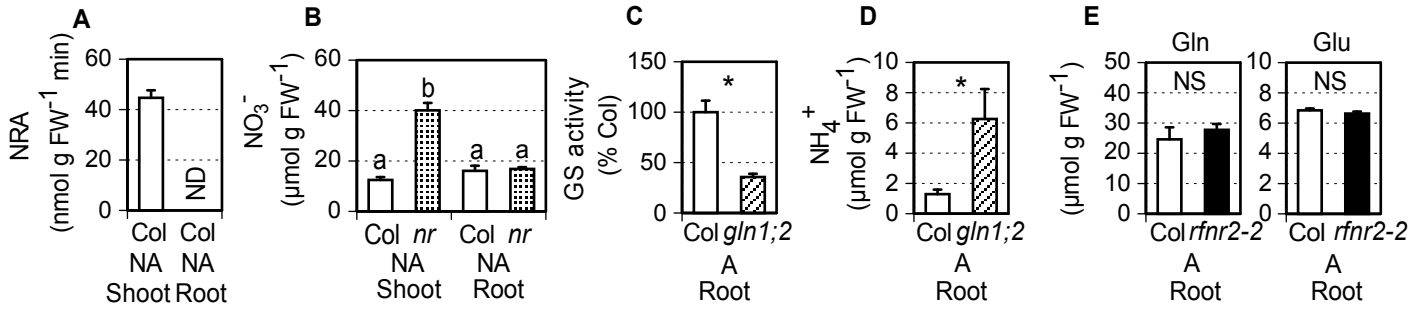**Table S1.** A list coexpressed with RFNR2 by ATTED II (Obayashi et al. 2007)

AGI No.	AGI No.	Gene name
1st	At1g24280	*G6PD3*
2nd	At5g41670	*dehydrogenase*
3rd	At5g13420	*TRA2*
4th	At4g05390	*RFNR1*
5th	At1g78050	*PGM*
6th	At5g13110	G6PD2
7th	At2g15620	*NIR*
8th	At1g63940	*MDAR6*
9th	At2g27510	*FD3*
10th	At1g64190	*dehydrogenase*

Table S2. Primer seqences

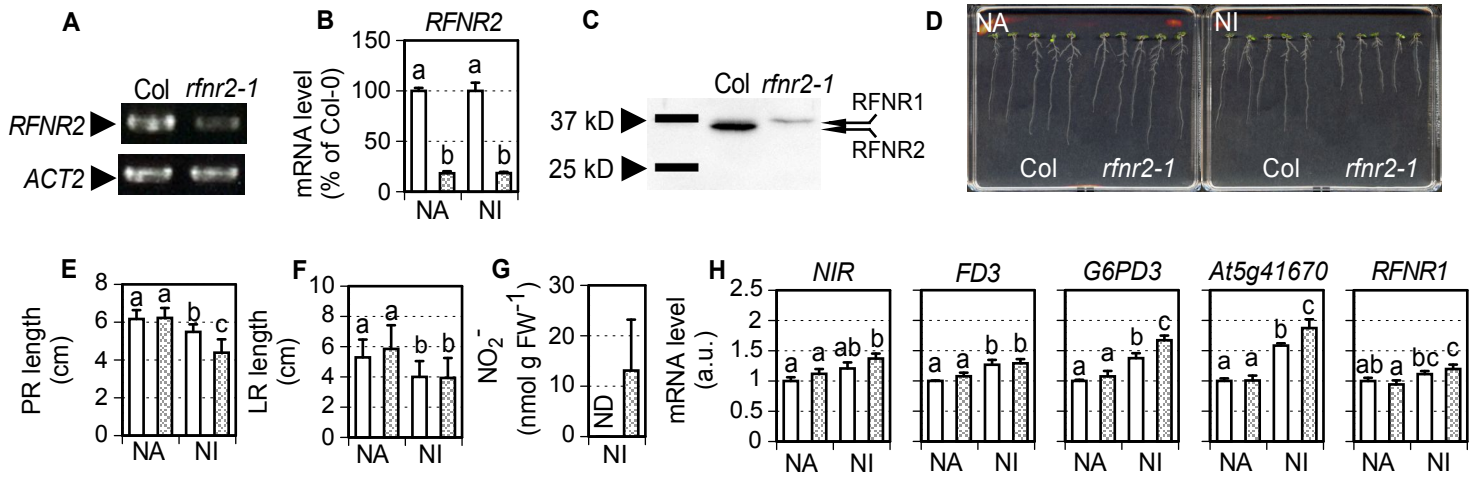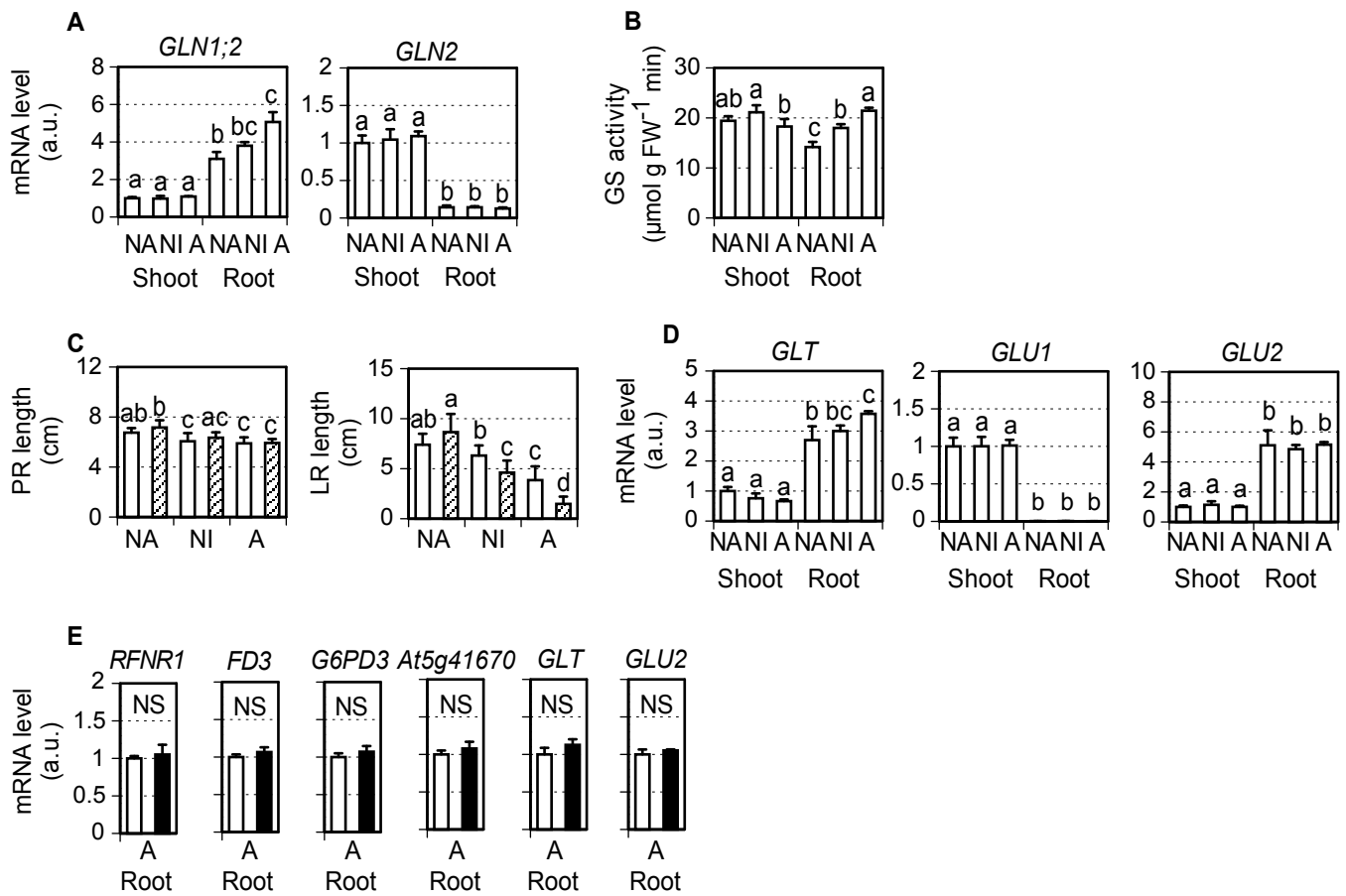| AGI No.	Gene name	Purpose	Primer 1 (5'->3')	Primer 2 (5'->3')	Reference
AT4G05390	RFNR1	gPCR for SALK_085009	TAACAACGAATTTGGCTTTGG	GGGATTCTCACCCTACGAGTC	This paper
AT1G30510	RFNR2	gPCR for SAIL_527_G10	CCAACTACTCGCTCCACAGAG	TCGGTTCAGGAAAATGATTTG	This paper
AT1G30510	RFNR2	gPCR for SALK_133654	TCAATAGACTTCAACGTGCCAC	CTCTGTGGAGCGAGTAGTTGG	This paper
AT3G18780	ACT2	RT-PCR/gPCR	TGTCCTCCTCACTTTCATCAGC	CATCAATTCGATCACTCAGAGC	This paper
AT4G05390	RFNR1	RT-PCR/gPCR	CACCATGGCTCTCTCAACTACTCCTTC	TCAATACACTTCAACATGCCACTGC	This paper
AT1G30510	RFNR2	RT-PCR/gPCR	CACCATGTCTCACTCTGCTGTTTC	TCAATAGACTTCAACGTGCCACTG	This paper
AT3G53750	ACT3	Q-PCR	GGCTAACCGTGAGAAGATGA	CGACCTGCAAGATCAAGACG	Watanabe et al. (2014)
AT3G22370	AOX1a	Q-PCR	CCGATTTGTTCTTCCAGAGG	GCGCTCTCTCGTACCATTTC	Escobar et al. (2004)
AT1G64190	At1g64190	Q-PCR	GCACTATCCCGAATCGGTCTC	AGGCGAGGTTTTGGCCCAT	This paper
AT4G34270	At4g34270	Q-PCR	CATTTCAGTCTCTATCTGCGAAAGGGTATCC	CACCACAATAAGTCAGTGGAGTAACTCCTTAC	Hong et al. (2010)
AT5G41670	At5g41670	Q-PCR	GAGTCAGTAAAGCATGGACACAGT	AGCTGAAACAATTTGTTTTCGTGTTCT	Gonzali et al. (2006)
AT2G27510	FD3	Q-PCR	GCAGCTGAAGAGGCAGGAGT	AAGTAGAACACGCACCGGCT	This paper
AT5G13110	G6PD2	Q-PCR	CCCTGGTTTAGGAATGAGAT	TAAGAGAAACCCCTTTGGTT	Wakao and Benning (2005)
AT1G24280	G6PD3	Q-PCR	TGGTTTATGGAAACTTTCTTTCGC	AGGGTGGCAAGAATAGGGTA	Ruffel et al. (2011)
AT1G66200	GLN1;2	Q-PCR	AGCCAAGCTTCTCGATCGCC	TGGAATGGAGCTGGTGCTCA	This paper
AT5G35630	GLN2	Q-PCR	TTGACCAGTTCTCATGGGGC	TTAGATGCTGGACGGCGATC	This paper
AT5G53460	GLT	Q-PCR	TTGGACCTGAGCCAACACTTG	CATCATCCGTTTTGGTGAGGA	Potel et al. (2009)
AT5G04140	GLU1	Q-PCR	ATCATTCAAGAGCAGGTTGT	GACAGTTGAAAGCAGTTATT	Potel et al. (2009)
AT2G41220	GLU2	Q-PCR	TACACATTTGATCGTGGTTT	AATCGAAAACCCTTTCTTAA	Potel et al. (2009)
-	GUS	Q-PCR	GAAAGCGCGTTACAAGAAAG	GACGTTGCCCGCATAATTAC	Tanabe et al. (2015)
AT5G66190	LFNR1	Q-PCR	CTGCAGTCTCTTTACCTTCTCC	GACAACAATCCCTTCTTCCTGTTTC	Lintala et al. (2009)
AT2G15620	NIR	Q-PCR	CATGGGATGCTTAACACGAG	AATGGAACCAACTCCGTGAC	Konishi and Yanagisawa (2011)
AT4G05390	RFNR1	Q-PCR	CAATGCCAAACCCGGCGATA	CCTTTCCAGATGGACCGGTGA	This paper
AT1G30510	RFNR2	Q-PCR	CGGGCTTTGAATCACATAGG	TGTGATTCCTCCAGGTGAGA	This paper

Figure S1

A

RFNR2 ▶
ACT2 ▶

Col rfnr2-1

B

RFNR2

C

Col rfnr2-1

37 kD ▶
25 kD ▶

RFNR1
RFNR2

D

E

F

G

H

NIR   *FD3*   *G6PD3*   *At5g41670*   *RFNR1*

Figure S2

Figure S3

A

B

C

D